Ultra Scientist Vol. 25(2)B, 193-220 (2013).

(Chadormalu iron oxide deposit, evidence for nonorogenic continental setting at Bafq region, central Iran)

A. MOGHTADERI*†

(Acceptance Date 10th May, 2013)

Abstract

Kiruna-type iron deposits are variable concentrations of magnetite-fluoroapatite-actinolite found in volcano-plutonic terranes from Early Proterozoic to Pliocene. No Archean ones are known. The iron ore deposits of Bafq region in central Iran have long been known as Kiruna-type. The origin and tectonic setting of these deposits have been a matter of debate during the last century. In this study, geochemistry of host rocks of Chadormalu and Esfordy iron deposits in Bafq region are investigated to elucidate the spatial-temporal characteristics of iron metallogeny. Geochemical evidence supports a nonorogenic continental setting. The Bafq region metallogenic characteristics are very similar to those of the Neoprotrozoic- Cambrian boundary.

Key words: Late-Proterozoic metallogeny, Iron oxide ore, Bafq region, Iran, Tectonic setting.

1. Introduction

In a global perspective, Kiruna-type iron deposits are variable concentrations of magnetitefluoroapatite- actinolite found in volcano-plutonic terranes from Early Proterozoic to the Pliocene[5,25,36,56,57,67,74]. No Archean representative is known[65,81]. The deposits consist of finegrained magnetite, or more rarely, hematite and contain variable amounts of apatite with accessory actinolite, epidote and diopside. The contact between the ore and the wall rocks is either gradational or sharp. Veinlets of ore extend both into the foot wall and the hanging wall. Magnetite and hematite ores form at deep and shallow levels, respectively. Iron oxide ores are generally hosted by intermediate to felsic volcanic rocks. The volcanic host is 4 to 6 km thick and iron mineralization occurs throughout the sequence. Dating reveals a temporal link between magmatism and iron mineralization[38].

* Corresponding author.Telefax:+98 7823624300
E-mail address: moghtaderiarsia2@yahoo.com (A. Moghtaderi)

Kiruna-type ore bodies are steep, pipe-like, or dike-like deposits, usually exhibiting a wide range of wall-rock alteration assemblages. Generally, the alteration display a general transition from sodic (albite-rich) alteration at deeper levels to potassic (potassium feldspar + sericite) alteration, to sericitic and silicic types in the uppermost portion of the system (sericite + quartz). Rare earth elements especially LREE are anomalous in both the iron ore and the commonly associated apatite[29,38,37]. Associated Au, Ag, Co, Ni, Te, and As mineralization is reported by some authors[3,38]. The best known and probably largest deposits are those found near Kiruna, Sweden[24,26], but other well-known deposits occur in Missouri[76], Chile[7], Bafq region-central Iran1[3,15,22,49,69,72,79] and at numerous locations around the Pacific ocean basin[58]. There is no worldwide consensus on the origin and tectonic setting of Kiruna-type deposits[8,24,55].

Current knowledge (*i.e.* lithological relationships, geometry, ore and gangue mineralogy, geological characteristics, *etc.*), places them within the magmatic-hydrothermal range (continuum). The majority of evidence from Kiruna-type deposits suggests they are basically products of hydrothermal processes occurring in the upper crust. Geologically, many deposits represent little direct evidence of magmatic process. Hydrothermal processes occur in both low and high temperature ranges. The low temperature deposits form on the floors of sedimentary basin by discharging ore forming fluids. The resultant synsedimetary iron ores are interstratified with the country rocks. The high temperature types which produce major orebodies form by hydrothermal-metasomatic processes on to preexisting rocks[11,12,13,20,23,27,37,38,49].

In this study, two iron-apatite deposits of Bafq region *i.e.* Chadormalu and Esfordy are investigated for a better understanding of spatial-temporal relationships of iron metallogeny at Bafq region.

2. Geology :

Bafq metallogenic province is located in central Iran about 115 Km Southeast of the Yazd city (55° 15′ – 55° 45′ E, 31° 30′ – 32° 30′ N) (Fig.1a-d).There are several known iron – phosphate, phosphate, Th-U and Pb-Zn deposits in the region. Recently, the occurrence of Cu-Au mineralization (probably porphyry in origin) is also reported[13]. The Bafq metallogenic province is part of the Lut block, composed of Precambrian continental basement covered with Late Proterozoic to Triassic sediments. During the Late Proterozoic Assyntic Orogeny the Precambrian basement of Iran and the neighboring Arabian shield consolidated and formed part of the Gondwanaland. The basement constitutes the rock units of the central Iranian continental terrane (Fig. 1a) with low to medium grade metamorphism, high level plutonic/volcanic rocks, and volcano-sedimentary formations composed of interbedded sequences of unmetamorphosed rhyolites and spilites with dolomitic limestones and minor evaporites. The magmatic rock suite consist of subvolcanic granites, minor andesites and diorites, rhyolitic lavas, pyroclastic rocks, "spilites'", late dolerites, and minor syenitic sills (albitites)[13,14,22,30].

According to Forster and Jafarzadeh[22] and Daliran[12,13], Bafq metallogenic province is a narrow paleorift extending northward from

south of Bafq town to and Robat- Posht– Badam (Fig. 1a). The age of the paleorift is suggested to be 750 – 540 Ma [11,30,33,70,71]. New U-Pb ages and geochemical data from magmatic, metamorphic and silisiclastic rocks of the Saqand-Bafq area[63] reveal three main episodes of orogenic activity in the late Neoprotrozoic-Early Cambrian, Late Triassic and Eocene. It is believed that, iron metallogeny occurred in the Early Cambrian (554-531.4 Ma ages). Paleontological evidence also supports a Lower Cambrian age for host rocks at Chadormalu iron oxide deposit[33]. The association of Bafq iron deposits with nonorogenic magmatism, continental margin or lacustrine halite facies evaporites, and lithological and mineralogical similarity with the red sea aborted rift deposits[37], indicate that Bafq iron deposits belong to an ancient failed rift.

Field investigations and remote sensing by several authors[6,12,13,20,22,46,69,70] revealed the presence of many curvilinear structures, faults and lineaments in Bafq metallogenic province.

The iron ores of the Bafq district are estimated to total 1500 million tones[13,22,51,53]. The deposits vary in size from small (20Mt, Mishdovan) to large 300-494 Mt (Choghart, Chadormalu and sechahun) ore bodies. The ore grade also varies from high (65% Fe), mostly, to low (20-30%Fe). Daliran[13] describes two main styles of deposition at Bafq region: (1) syngenetic submarine hydrothermal deposits, generated by discharge of ore fluids into a sedimentary basin (e.g., Mishdovan and Narigan). (2) epigenetic replacement deposits formed by the penetration of the ore fluids into sub – volcanic and volcanic rhyolitic rocks (e.g. Choghart, Chadermalu and northern anomaly). The latter is usually associated with massive apatite – magnetite – hematite ores.

The Chadormalu deposit (55° 30' E, 32° 17' N) which was first discovered by Kumel in 1941 [22], is the largest known iron ore deposit in Iran (Fig.1b). It includes the northern gravity anomaly, the northern ore body, the southern ore body and the southern gravity anomaly. The ore bodies are arranged in the north-northeast-south-southwest direction along the eastern segment of the ring fracture of the Kuh-e-Sorkh caldera[22]. The eastern caldera rim consists of metamorphic rocks (Fig. 1c). Jafarzadeh[41], and Forster and Jafarzadeh[21,22] propose that the Chadormalu iron deposit is a magnetite – filled vent, more than 600 m deep. The northern orebody is a vertical cylinder with several horizontal extensions. The southern orebody is a tabular lens, derived from a ring graben trending SSW. According to field observations, the host rocks are diorite-phenoandesite, metamorphic rocks, subvolcanic intrusive syenite, hornblendite-pyroxenite, volcanic rocks (rhyolite, andesite) and pyroclastic fill of the vent. The resurgent Zarigan granite contains metamorphosed xenoliths of the country rocks (Fig. 1c). Rhyolite is albitized several meters from the contact of the massive magnetite ore[22].

The Esfordy (apatite-iron) deposit (Fig. 1b, d) is located in the Bafq metallogenic province in central Iran, about 36 Km northeast of Bafq town (55° 38' E, 31° 15' N). Magmatically, there is a wide range of igneous rocks, including, porphyry quartz, rhyolite, syenite, monzonite, andesite basalt and Zarigan granite (bimodal composition). Sedimentary rocks

include cherty brown dolomite, green shale, sandstone, slaty shale, graywack, conglomerate and limestone. Quartzite is dominant metamorphic rock. Most of lithological unit contacts are fault controlled[31].

3. Methodology :

In order to draw a probable tectonic environment, some fresh and slightly altered host rocks from Chadormalu deposit were sampled and analyzed. The results were compared with published Chadormalu[63], and Esfordy[40] data. Whole-rock chemistry was determined using XRF spectrography; Ba and Ta were determined by ICP (Amdel lab, Australia).

Sm-Nd analyses were carried out in the isotope lab, Faculty of Earth Sciences China University of Geosciences. Sample preparation included digestion, using standard methods and chemical separation and purification of Nd and Sm. Sm and Nd isotopic ratios for individual samples are calculated using their measured Sm and Nd content in spiked mixture with ^{149}Sm and ^{145}Nd isotopic tracers.

Two aliquots, about 50 milligrams, are weighted from the powder (200 meshes) of each sample. Some mixture solution of ^{149}Sm and ^{145}Nd isotopic spikes is weighted and added into one of the aliquot for every sample. Samples are held in screw top PTFE-lined stainless steel bombs with an acid mixture of 1 ml: 1ml concentrated HF, and HNO_3. The sealed bombs were put into an electronic oven at 185°C for 48 hours for digestion. Decomposed samples were dried on a hot plate, and chlorinated by adding acids of concentrated $HClO_4$ and HCl orderly. The re-dried salts of the samples are re-dissolved into 500-1500 microlitres (µl) solutions of 2.5N HCl acid. After centrifuging, the clean solutions were loaded into columns of AG50W-X12 and HDEHP (LN resin of Eichrom technologies Inc.) resins sequentially for separation and purification of REE, Nd and Sm respectively by HCl eluants. The purified Nd- and Sm- bearing solutions are dried and ready for their isotopic analysis by TIMS (Thermal Ionization Mass Spectrometer) of Triton Ti, Finnigan of THEROM.

Sm and Nd contents and their isotopic ratios for individual samples are calculated according to their measured Sm and Nd isotopic ratios in their spiked mixture with ^{149}Sm and ^{145}Nd isotopic tracers, together with the weights of sample's powder and spike solution. Nd isotopic ratios of each sample are measured from the spike-free aliquot. The 143Nd/144Nd ratio are normalized by $^{146}Nd/^{144}Nd=0.721900$.

During the run of samples, the TIMS in this lab gave a ratio of $^{143}Nd/^{144}Nd$ for LaJolla standard solution of 0.511847±0.000003 (n=2). And yielded values of 27.99 ppm, 6.703 ppm and 0.512626±0.000003 of Nd, Sm contents and $^{143}Nd/^{144}Nd$ ratio respectively for the standard material of BCR-2 basalt. The whole-procedure blanks are about 200 pg and 25 pg for Nd and Sm respectively.

Allegre *et al*.[2] normalizing parameters were used in dating. The results of major and trace element analysis are listed in table 1a-d. Sample description and locations are given in table. 2. The Sm-Nd model age results are also presented in Table. 3. The geochemical diagrams are prepared using Minpet 2.02 software.

Ramezani and Tucker[63] and Hamdi[33], proposed an Early-Cambrian age for the volcano-sedimentary host rocks of Bafq region, including, Chadormalu deposit. The former authors suggested an extensional arc environment for this region based on Rb-Y-Nb, Rb-Y-Ta and Th-Hf-Ta diagrams. As both Hf and Ta are highly mobile during low to high temperature alterations and can not be accurately measured by XRF spectrography[66] the normally used Rb-Y-Nb, Rb-Y-Ta and Th-Hf-Ta diagrams for tectonic setting determination[61,82] were not used in this study. Furthermore, the volcanic wall rocks of Bafq iron deposits are pervasively altered[30,47]. Altered and fresh host rocks were discriminated (Table 2) using Taylor and Fryer[77] method along with field and petrographic investigations.

4. Data interpretation :

The host rocks of Chadormalu area according to this study and the study conducted by Ramezani and Tucker[63] and also the Esfordy data[40], vary from sub-alkaline basalt, through, basalt-andesite, andesite/basalt, Rhyodacite/ dacite, trachy andesite to rhyolite; basic diorite, alkali granite to sodic phonolite; indicating an alkaline-sub alkaline or a bimodal composition (fig. 2a, b and fig. 3a-d). Harker diagrams represent a magmatic suit at Chadormalu deposit (fig. 4a, b). The tectonic setting diagrams (Fig. 5a, b) illustrate a within plate setting. Ti-Zr-Y diagram[59] suggests a within plate basaltic (D domain) environment. In the Zr/Y-Zr [62], the plotted rocks also indicate a within plate basalt. Meschede's diagram[44] discriminate the samples as within plate alkali-basalts (AI) tholiites (AI, C) and MORB (D). The MgO-FeO-Al2O3 diagram[60] which is commonly used to discriminate sub alkaline basalts and basaltic-andesites (SiO2 wt%= 51-56),[66], suggests a continental environment (Fig. 5 a, b). However, some Chadormalu samples do not fit in to the continental field, probably due to relative mobility of major elements or crystal fractionation[66].

Boron is an interesting trace element as it is strongly enriched in seawater and marine sediments compared with it's concentration in most crust and mantle rock types. Therefore, boron can be used as a tracer to indicate the presence of subducted sediment or altered oceanic crust in magmas source regions. Boron concentration generally varies between 1 to 2 ppm in mid-ocean ridges and ocean island basalts, but, frequently reaches to more than 10 ppm in volcanic arc basalts and andesites[32,68]. No boron was detected in this study or those conducted by Ramezani and Tucker[63] and Isfahani and Sharifi[40] probably indicating an orogenic continental rift setting in Bafq region.

The depleted mantle (DM) model age suggest 1.1-1.3 Ga (Riphean stage) for Chadormalu deposit (host rock and ore), indicating that the igneous host rocks and iron ores are temporally (and hence spatially) related.

According to Nohda and Wasserburge [54] and Davidson[16], radiogenic isotope results at Chadormalu deposit (table 3) represent continental environments, mantle (end of mantle array) source (host rock) and crustal origin (iron ores) deposit with some crustal contamination at Chadormalu. The authors suggested that $^{143}Nd/^{144}Nd$ ratio is 0.5122-0.5134 in

Table. 1a-d.

The results of major and trace element analysis of Chadormalu (CHD, this study), and Bafq region (JR, BFQ); from Isfahani and Sharifi [40]; Ramezani and Tucker [63]. Ba, B, and Ta (CHD codes) were analyzed by IC3E technique; Au element has been analyzed by Fire assay technique (CHD codes), another samples analyzed by XRF technique. Detection limits of major elements in this study (CHD codes) are 0.01wt%, except, TiO_2, MnO and P_2O_5 have 0.001wt%. The detection limits of trace elements (except Ba, B, Ta and Au) are 1ppm. Detection of B element is 0.5 ppm. Au detection is 1ppb. Ba and Ta detections are 0.2 and 0.1 respectively. ND = Not Detected.

	SiO_2 wt%	TiO_2 wt%	Al_2O_3 wt%	Fe_2O_3 wt%	FeO wt%	FeOT wt%	Fe_2O_3T wt%	MnO wt%	MgO wt%	CaO wt%	Na_2O wt%	K_2O wt%	P_2O_5 wt%
BFQ508	72.4	0.14	11.2	0.54	0.14	0.63	0.7	0.06	0.94	2.8	0.13	9.38	0
BFQ509	68.5	0.27	10.52	7.65	0.31	7.19	7.99	0.1	2.41	0.09	0.21	9.46	0.17
BFQ510	71.3	0.09	12.1	0.48	0.43	0.86	0.96	0.09	0.44	1.31	0.15	11.46	0.12
BFQ511	69.18	0.2	11.98	0.56	0.66	1.16	1.29	0.04	2.85	2.24	0.14	8.45	0
BFQ513	48	0.75	15.25	4.27	3.85	7.69	8.55	0.24	12.74	6.79	2.65	1.45	0.38
BFQ515	70.6	0.38	14.34	0.51	2.24	2.7	3	0.06	3.43	1.95	3.05	2.2	0.25
JR94-G14	65.91	0.69	14.57	4.08	0.46	4.13	4.59	0.06	2.1	3.43	3.03	4.21	0.16
JR94-G16	71.31	0.32	14.65	2.6	0.4	2.74	3.04	0.04	0.57	1.92	3.87	3.23	0.09
JR94-G17	75.77	0.02	13.35	0.97	0.11	0.98	1.09	0.05	0.09	0.7	3.57	4.52	0.02
JR94-G28	79.06	0.24	11.95	0.13	0.02	0.14	0.15	0.01	0.19	0.45	6.22	1.46	0.08
JR95-A40	73.93	0.25	13.01	2.23	0.25	2.26	2.51	0.06	0.41	1.36	3.37	3.97	0.05
JR95-G37	73.3	0.28	13.41	2.59	0.29	2.62	2.91	0.05	0.64	1.29	3.69	3.32	0.09
JR95-G39	76.15	0.18	12.68	1.32	0.15	1.34	1.49	0.02	0.17	0.48	4.22	4.92	0.01
JR95-G47	67.05	0.81	13.23	6.48	0.73	6.56	7.29	0.05	0.47	1.76	6.48	1.7	0.21
JR95-G50	71.81	0.31	19.09	2.69	0.3	2.72	3.02	0.07	0.63	2.24	3.01	3.96	0.11
JR95-G54	68.81	0.52	14.56	3.77	0.42	3.81	4.24	0.06	1.4	3.57	3.58	2.86	0.08
JR95-G55	76.26	0.16	12.57	11.31	1.26	11.44	12.71	0.01	0.25	1.06	3.47	3.47	0.01
CHD-1	78.65	0.122	11.8	0.98	0.11	0.99	1.1	0.007	0.19	0.78	6.3	0.04	0.015
CHD-11	56.85	1.769	11.14	11.16	1.25	11.29	12.55	0.168	4.65	5.56	3.88	0.08	0.959
CHD-12	52.88	2.488	10.63	12.11	1.34	12.24	13.6	0.166	6.96	4.96	2.08	0.67	0.86
CHD-13	51.95	2.516	13.21	13.64	1.52	13.79	15.33	0.129	5.67	3.33	3.91	0.19	0.678
CHD-16	49.65	1.799	10.65	8.15	0.91	8.24	9.16	0.242	5.68	8.63	2.92	0.57	0.947
CHD-18	37.8	0.542	9.26	4.26	0.47	4.3	4.78	0.091	3.31	21.23	0.94	0.95	0.113
CHD-21	60.56	0.121	7.11	3.25	0.37	3.29	3.66	0.052	8.19	9.48	2.09	1.09	0.021
CHD-22	63.11	0.093	7.02	7.01	0.79	7.1	7.89	0.065	10.55	6.03	2.39	0.92	0.017
CHD-3	77.56	0.146	11.63	1.57	0.17	1.58	1.76	0.011	0.41	1	5.37	0.19	0.017
CHD-50	77.22	0.205	12.1	2.27	0.26	2.3	2.56	0.005	0.26	0.45	6.32	0.08	0.052
CHD-55	75.1	0.707	13.65	1.02	0.12	1.04	1.15	0.026	0.49	1.25	6.44	0.4	0.103
CHD-56	65.56	0.802	13.24	3.1	0.35	3.14	3.49	0.139	1.83	3.62	2.95	2.81	0.16
CHD-6	55.84	2.38	10.87	11.067	1.233	11.19	12.44	0.172	4.94	5.97	3.37	0.19	0.987
CHD-60	41.16	9.493	1.71	20.14	0.25	18.37	20.42	0.067	18.05	2.45	0.01	0.26	0.01

Table 1b.

Sample	H_2O_p	LOI	ACNK	Cl	Ba	Rb	Sr	Y	Zr	Nb	Th	Ga	Zn	Cu
	wt%	wt%		(ppm)	(ppm)	(ppm)	(ppm)	(ppm)	(ppm)	(ppm)	(ppm)	(ppm)	(ppm)	(ppm)
BFQ508	2.68	0	ND	ND	ND	ND	ND	ND	ND	ND	ND	ND	ND	ND
BFQ509	0.75	0	ND	ND	ND	ND	ND	ND	ND	ND	ND	ND	ND	ND
BFQ510	0.42	0	ND	ND	ND	ND	ND	ND	ND	ND	ND	ND	ND	ND
BFQ511	1.01	0	ND	ND	ND	ND	ND	ND	ND	ND	ND	ND	ND	ND
BFQ513	5.03	0	ND	ND	ND	ND	ND	ND	ND	ND	ND	ND	ND	ND
BFQ515	0.73	0	ND	ND	ND	ND	ND	ND	ND	ND	ND	ND	ND	ND
JR94G14	ND	1.41	ND	ND	644	131	184	25	262	15.7	0	16	64	ND
JR94G16	ND	1.11	ND	ND	732	117	152	16	147	10.4	12.29	18	50	ND
JR94G17	ND	0.53	ND	ND	447	163	51	34	66	12.7	ND	17	42	ND
JR94G28	ND	0.57	ND	ND	154	18	26	26	125	2.4	5.82	7	2	ND
JR95A40	ND	0.97	ND	ND	502	153	84	22	132	10.8	17.55	14	42	ND
JR95G37	ND	1.42	ND	ND	602	121	140	21	122	8.8	12.32	16	24	ND
JR95G39	ND	0.39	ND	ND	659	51	38	14	191	2.9	13.32	15	16	ND
JR95G47	ND	0.93	ND	ND	205	16	56	114	850	22.7	8.41	29	19	ND
JR95G50	ND	0.67	ND	ND	787	162	221	16	165	15.6	24	14	61	ND
JR95G54	ND	0.62	ND	ND	868	83	171	27	200	7.4	8.61	17	38	ND
JR95G55	ND	0.41	ND	ND	648	114	77	24	118	7.6	18.36	13	12	ND
CHD-1	ND	0.66	63	0.0062	6	29	35	189	14	15	5	10	1	2
CHD-11	ND	2.26	89	0.0473	6	65	27	231	2	2	2	71	1	24
CHD-12	ND	4.47	117	0.0699	29	64	25	166	3	8	4	79	1	7
CHD-13	ND	2.85	153	0.0446	14	58	33	372	21	5	2	55	83	7
CHD-16	ND	9.52	11	0.0338	18	74	27	183	6	3	6	26	1	14
CHD-18	ND	20.59	207	0.0528	31	68	17	106	7	8	14	34	1	14
CHD-21	ND	7.24	2	0.0159	24	47	57	135	2	10	5	31	1	19
CHD-22	ND	1.56	29	0.0295	29	20	48	126	4	13	1	32	1	24
CHD-3	ND	1.62	79	0.0052	9	39	36	190	12	17	2	23	1	6
CHD-50	ND	0.39	143	0.0159	7	20	10	164	8	8	5	18	57	2
CHD-55	ND	5.06	366	0.0243	14	44	22	150	3	24	8	14	1	4
CHD-56	ND	5.06	366	0.0243	50	54	28	224	7	8	6	16	1	6
CHD-6	ND	2.62	149	0.0436	9	53	27	192	ND	3	4	70	2	6
CHD-60	ND	4.13	256	0.0313	13	15	23	27	61	9	1	23	1	56

Table 1c.

Sample	Ni (ppm)	V (ppm)	Cr (ppm)	Hf (ppm)	Cs (ppm)	Sc (ppm)	Ta (ppm)	Co (ppm)	B (ppm)	XCl	U (ppm)	Sn (ppm)
BFQ508	ND	ND	ND	ND	ND	ND	ND	ND	ND	ND	ND	ND
BFQ509	ND	ND	ND	ND	ND	ND	ND	ND	ND	ND	ND	ND
BFQ510	ND	ND	ND	ND	ND	ND	ND	ND	ND	ND	ND	ND
BFQ511	ND	ND	ND	ND	ND	ND	ND	ND	ND	ND	ND	ND
BFQ513	ND	ND	ND	ND	ND	ND	ND	ND	ND	ND	ND	ND
BFQ515	ND	ND	ND	ND	ND	ND	ND	ND	ND	ND	ND	ND
JR94-G14	22	82	75	ND	ND	ND	ND	11	0	ND	ND	8.3
JR94-G16	2	25	2	4.48	7.61	6	0.8	4	0	ND	2.21	7.9
JR94-G17	6	ND	8	ND	ND	ND	ND	4	ND	ND	ND	6.7
JR94-G28	4	6	2	3.53	0.07	3	0.38	10	0	ND	2.32	5.9
JR95-A40	ND	17	2	4.34	6.86	5	1.07	3	0	ND	3.36	5
JR95-G37	ND	25	2	4.32	1.7	7	0.91	3	0	ND	2.92	4.7
JR95-G39	ND	5	1	7.15	0.23	3	0.3	3	0	ND	1.93	3
JR95-G47	ND	14	1	23	0.15	11	1.55	3	0	ND	2.37	14.3
JR95-G50	ND	15	3	4.68	6.29	5	1.24	4	0	ND	2.65	4.9
JR95-G54	9	70	18	5.89	1.83	13	0.49	8	0	ND	0.97	4.2
JR95-G55	ND	10	2	4.75	1.05	3	0.93	2	0	ND	3.64	5.3
CHD-1	24	2	ND	ND	ND	ND	2	ND	0	5	1	1
CHD-11	193	36	ND	0.1	ND	ND	23	ND	0	9	1	4
CHD-12	309	14	ND	ND	ND	ND	18	ND	0	7	1	4
CHD-13	232	4	ND	ND	ND	ND	19	ND	0	1	6	5
CHD-16	186	5	ND	ND	ND	ND	23	ND	0	1	1	6
CHD-18	48	15	ND	ND	ND	ND	6	ND	0	1	1	7
CHD-21	78	1	ND	ND	ND	ND	4	ND	0	7	1	2
CHD-22	72	1	ND	ND	ND	ND	15	ND	0	4	3	5
CHD-3	21	3	ND	ND	ND	ND	5	ND	0	5	4	2
CHD-50	44	2	ND	ND	ND	ND	17	ND	0	4	4	3
CHD-55	44	26	ND	ND	ND	ND	6	ND	0	3	1	1
CHD-56	74	9	ND	ND	ND	ND	2	ND	0	4	1	2
CHD-6	280	9	ND	ND	ND	ND	23	ND	0	3	2	3
CHD-60	1159	2152	ND	ND	ND	ND	56	ND	0	5	1	8

Table. 1d.

	Au (ppm)	La (ppm)	Ce (ppm)	Pr (ppm)	Nd (ppm)	Sm (ppm)	Eu (ppm)	Gd (ppm)	Tb (ppm)	Dy (ppm)	Ho (ppm)	Er (ppm)	Tm (ppm)	Yb (ppm)	Lu (ppm)
BFQ508	ND	ND	ND	ND	ND	ND	ND	ND	ND	ND	ND	ND	ND	ND	ND
BFQ509	ND	ND	ND	ND	ND	ND	ND	ND	ND	ND	ND	ND	ND	ND	ND
BFQ510	ND	ND	ND	ND	ND	ND	ND	ND	ND	ND	ND	ND	ND	ND	ND
BFQ511	ND	ND	ND	ND	ND	ND	ND	ND	ND	ND	ND	ND	ND	ND	ND
BFQ513	ND	ND	ND	ND	ND	ND	ND	ND	ND	ND	ND	ND	ND	ND	ND
BFQ515	ND	ND	ND	ND	ND	ND	ND	ND	ND	ND	ND	ND	ND	ND	ND
JR94-G14	ND	ND	ND	ND	ND	ND	ND	ND	ND	ND	ND	ND	ND	ND	ND
JR94-G16	ND	34.3	64.2	6.48	21.3	4.08	0.77	3.42	0.49	ND	ND	ND	ND	1.54	0.24
JR94-G17	ND	ND	ND	ND	ND	ND	ND	ND	ND	ND	ND	ND	ND	ND	ND
JR94-G28	ND	30.2	57.2	6.28	22.4	4.06	0.89	4.22	0.67	ND	ND	ND	ND	2.47	0.36
JR95-A40	ND	32.6	63.7	6.68	22.8	4.58	0.59	4.15	0.62	ND	ND	ND	ND	2.14	0.31
JR95-G37	ND	26.8	50.1	5.32	18.4	3.96	0.66	3.91	0.61	ND	ND	ND	ND	2.36	0.34
JR95-G39	ND	44.8	88.4	9.44	32.8	4.97	0.7	3.65	0.49	ND	ND	ND	ND	1.65	0.25
JR95-G47	ND	57.8	135.2	16.69	67	17.82	3.92	20.1	3.34	ND	ND	ND	ND	13.7	2.05
JR95-G50	ND	57.8	113.6	11.85	40.2	6.56	1.13	4.3	0.55	ND	ND	ND	ND	1.49	0.23
JR95-G54	ND	34.4	67.2	7.51	27.3	5.59	1.06	5.37	0.82	ND	ND	ND	ND	2.8	0.4
JR95-G55	ND	34.4	62.5	6.28	20.5	3.92	0.55	3.88	0.6	ND	ND	ND	ND	3.12	0.47
CHD-1	17	51.7	8.3	50.5	7.51	0.53	6.45	0.56	2.19	0.42	1.32	0.28	1.92	0.34	ND
CHD-11	ND	ND	ND	ND	ND	ND	ND	ND	ND	ND	ND	ND	ND	ND	ND
CHD-12	17	71.6	9.85	65.6	11.5	3.52	16.6	2.16	11	16.6	5.55	0.71	4.33	0.48	ND
CHD-13	ND	ND	ND	ND	ND	ND	ND	ND	ND	ND	ND	ND	ND	ND	ND
CHD-16	24	64.1	10.5	64.1	9.53	2.58	11.5	1.26	5.82	0.99	2.52	0.3	1.8	0.22	ND
CHD-18	23	55.8	6.55	34.2	4.35	0.74	4.3	0.49	2.43	0.45	1.36	0.21	1.58	0.2	ND
CHD-21	31	107	16.9	99	13.7	0.84	11.4	1.35	6.61	1.33	3.68	0.57	4.35	0.6	ND
CHD-22	112	356	52.8	286	47.9	4.48	45.8	4.63	17.7	2.46	6.67	0.96	7.58	1.11	ND
CHD-3	ND	ND	ND	ND	ND	ND	ND	ND	ND	ND	ND	ND	ND	ND	ND
CHD-50	3.32	9.35	0.91	3.56	0.7	0.25	0.64	0.13	0.97	0.2	0.7	0.1	0.62	0.08	ND
CHD-55	20.2	52.9	8.07	36.1	7.28	0.92	3.14	0.37	1.63	0.24	0.73	0.1	0.67	0.08	ND
CHD-56	ND	ND	ND	ND	ND	ND	ND	ND	ND	ND	ND	ND	ND	ND	ND
CHD-6	ND	ND	ND	ND	ND	ND	ND	ND	ND	ND	ND	ND	ND	ND	ND
CHD-60	42.6	79.9	14	68.5	13.7	1.34	9.44	1.75	11.3	2.08	6.5	1.03	6.75	0.87	ND

Table. 2. Locations and descriptions of samples

Sample	Coordination(UTM/ DEG,SEC)	Alteration type
CHD-1	3574089N, 360409E	Potassic
CHD-11	3573443N, 360268E	Fresh
CHD-12	3574183N, 360268E	Fresh
CHD-13	3574281N, 360190E	Enriched in Zr and Nb.
CHD-16	3574679N, 360304E	Fresh
CHD-18	3574731N, 360522E	Minor depleted in Zr, Enriched in Nb.
CHD-21	3574335N, 360253E	Fresh
CHD-22	3574580N, 360305E	Fresh
CHD-3	3574061N, 360323E	Fresh
CHD-50	3574092N, 360299E	Potassic
CHD-55	3574281N, 360190E	Sodic
CHD-56	3574507N, 360166E	Potassic
CHD-6	3574061N, 360323E	Fresh
CHD-60	3574459N, 360237E	Fresh
BFQ-508	31º 48’N, 55º 35’E	Fresh
BFQ-509	31º 48’N, 55º 35’E	Fresh
BFQ-510	31º 48’N, 55º 35’E	Fresh
BFQ-511	31º 48’N, 55º 35’E	Fresh
BFQ-513	31º 48’N, 55º 35’E	Fresh
BFQ-515	33º 09’N, 55º 33’E	Fresh
JR94-G14	ND	Enriched in Ni, Zr, Y, Nb, Rb.
JR94-G16	ND	Enriched in Sr, Nb, Rb.
JR94-G17	ND	Depleted in Zr, Enriched in Ba, Nb, Rb, Sr.
JR94-G28	ND	Fresh
JR95-A40	ND	Fresh
JR95-G37	ND	Fresh
JR95-G39	ND	Depleted in Y, Enriched in Nb, Zr, Sr, Rb, Ba, Cs.
JR95-G47	ND	Depleted in Rb, Enriched in Zr, Y, Nb, Sr, Ba, Cs.
JR95-G50	ND	Depleted in Y, Enriched in Cs, Nb, Sr, Rb, Ba.
JR95-G54	ND	Fresh
JR95-G55	ND	Fresh

Table. 3. The results of Sm-Nd dating at Chadermalu host rocks and ore minerals (magnetite and hematite)

Sample	143Nd/ 144Nd	147Sm/ 144Nd	Nd, ppm	Sm, ppm	T (DM)	ε Nd	SD Err (2s,10-6)
1450-5C	0.512202	0.1138	87.50	16.47	1.19 Ga	-85.05	1
1435-11C	0.512176	0.0985	97.28	15.84	1.17 Ga	-90.12	2
SA3	0.512186	0.1081	67.81	12.12	1.36 Ga	-88.17	2
1435-14C	0.512195	0.0984	37.78	6.15	1.10 Ga	-86.41	2
1465-12C	0.512692	0.1590	51.11	13.45	1.01 Ga	+10.5	2
1420-1C	0.512694	0.1724	39.41	11.24	1.17 Ga	+10.92	2
1480-7C	0.512369	0.1443	81.23	19.39	1.34 Ga	-52.47	1
1480-9C	0.512731	0.1771	47.12	13.80	1.17 Ga	+18.14	3
1495-3C	0.512752	0.1637	52.27	14.15	0.95 Ga	+21.8	2

Notes: 1420-1C, 1465-12C, 1480-7C, 1480-9C, 1495-3C stand for andesitic rocks. 1435-11C, 1435-14C, 1450-5C, and SA3 stand for magnetite ores.

continental rift basic rocks (end of mantle array source) or continental rift volcanism. Also positive and negative contents of ɛNd in table 3 indicate mantle and crustal source, respectively.

5. Discussion and Conclusion

Hitzman[37] suggested three tectonic environments in which iron oxide (Cu-U-Au-REE) deposits can form: A) intra-continental orogenic collapse B) intra-continental anorogenic magmatism C) extension along a subduction related continental margin.; all these environments have important voluminous igneous activity probably related to mantle underplating, high heat flow and source rocks (subaerial basalts, sediments, evaporites and/or magmas that are relatively oxidized). Deposits that are associated with anorogenic magmatism (B-type) generally contain voluminous felsic intrusive and extrusive rocks with lesser mafic igneous rocks. The rock compositions are variable ranging from rhyolites and granites through andesites to basalts and gabbros (bimodalcomposition). The felsic extrusive rocks are the result of voluminous caldera eruptions. They have calc-alkaline or alkaline to sub alkaline-alkaline nature. Many are identified as syenites and/or red granite (e.g. Sorkh granite in the vicinity of Chadormalu paleocrater) (Fig. 1c); these rocks generally display either potassic or sodic alteration and are pervasively replaced by hydrothermal hematite and magnetite. Extensive sodic, potassic, sericitic, slicic alterations are already noted at Chadormalu paleocrater and its associated iron deposit[47]. Sedimentary rocks

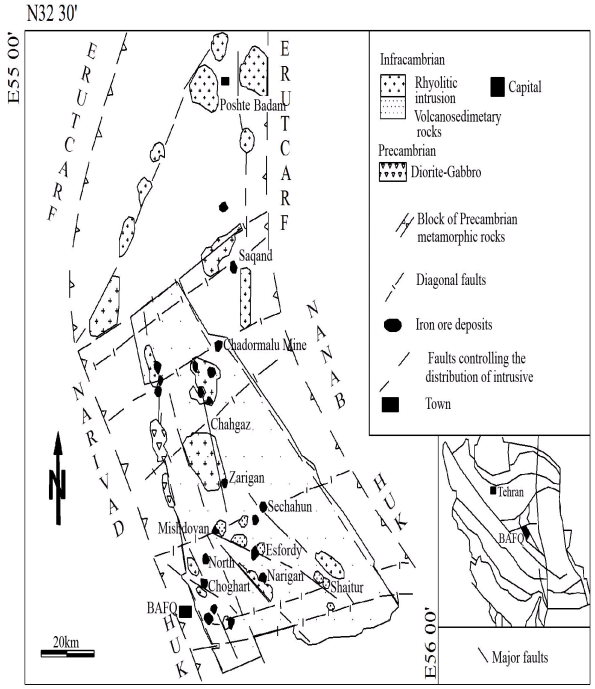

Fig. 1a

Fig. 1(a) Bafq paleorift and iron deposits. Many deposits are elongated parallel to regional or local structural trends and are hosted by rhyolitic rocks (modified from Daliran, [13]) (b) Location of Chadormalu and Esfordy mines in Bafq region (c, d) Geological maps of Chadormalu and Esfordy mines.

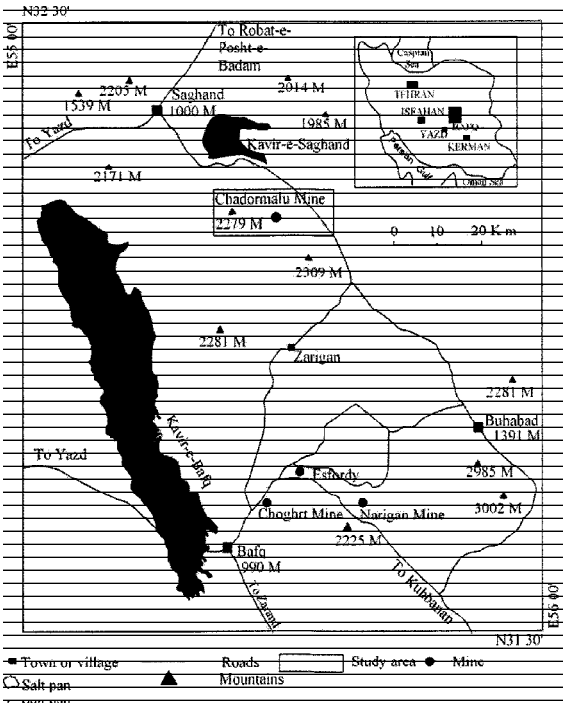

Fig. 1b

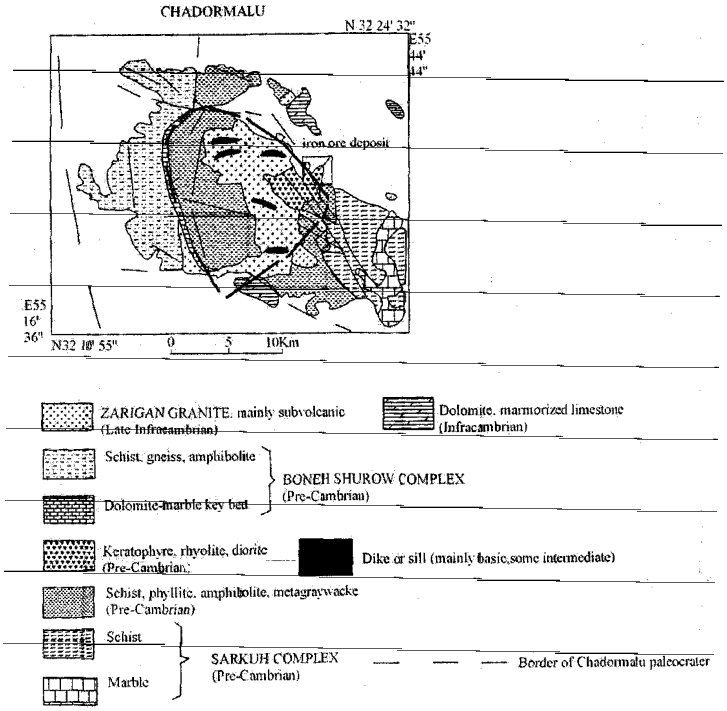
CHADORMALU
N 32 24' 32"
E55
44'
44"
iron ore deposit
E55
16'
36"
N32 18' 55"
0
5
10Km
ZARIGAN GRANITE, mainly subvolcanic
(Late Infracambrian)
Dolomite, marmorized limestone
(Infracambrian)
Schist, gneiss, amphibolite
Dolomite-marble key bed
BONEH SHUROW COMPLEX
(Pre-Cambrian)
Keratophyre, rhyolite, diorite
(Pre-Cambrian)
Dike or sill (mainly basic,some intermediate)
Schist, phyllite, amphibolite, metagraywacke
(Pre-Cambrian)
Schist
Marble
SARKUH COMPLEX
(Pre-Cambrian)
Border of Chadormalu paleocrater

Fig. 1c

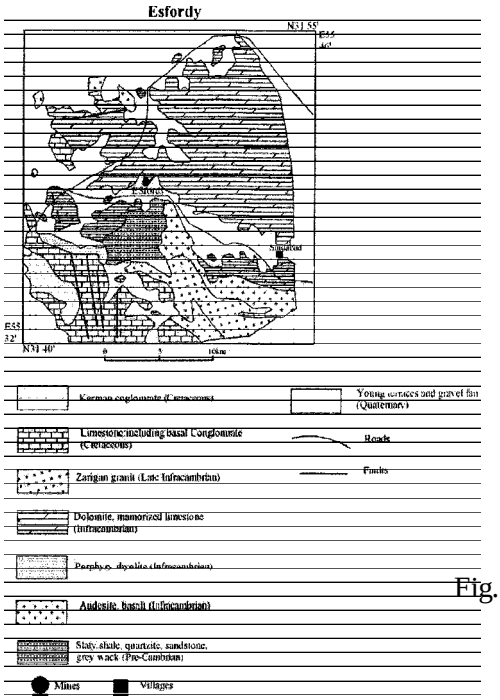
Esfordy
N31 55'
E55
46'
E55
32'
N31 40'
0
5
10km
Limestone including basal Conglomerate
(Cretaceous)
Zarigan granit (Late Infracambrian)
Dolomite, mamorized limestone
(Infracambrian)
Andesite, basalt (Infracambrian)
Slaty, shale, quartzite, sandstone,
grey wack (Pre-Cambrian)
Young terraces and gravel fan
(Quaternary)
Roads
Faults
Mines
Villages

Fig. 1d

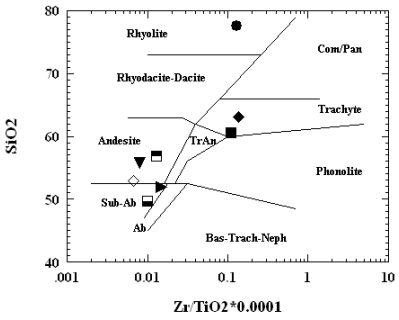

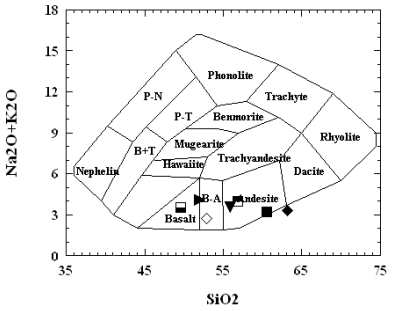

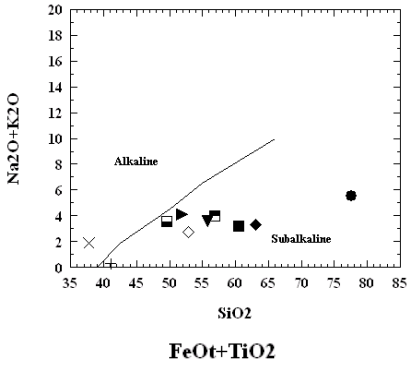

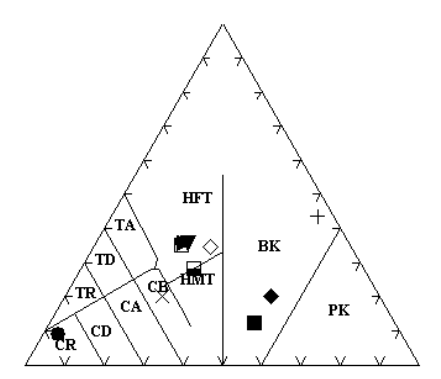

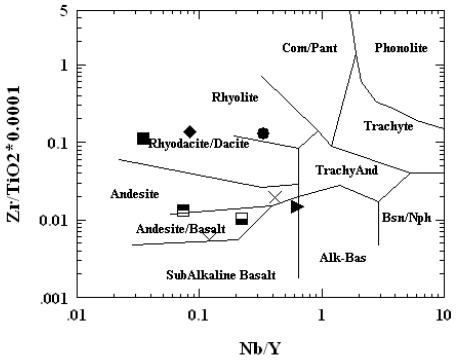

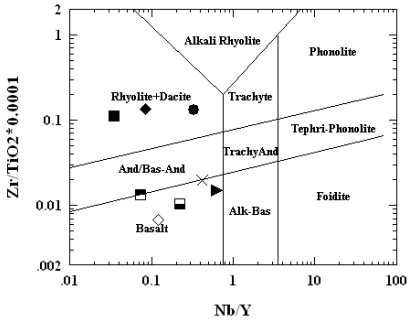

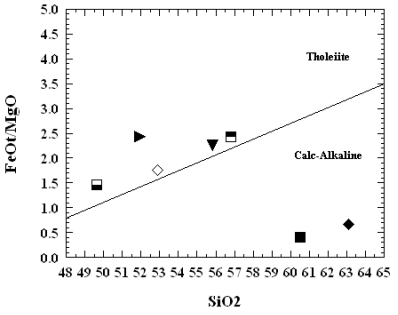

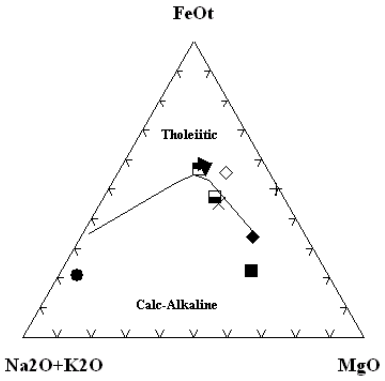

Fig. 2 (a) Rock types, compositions and series at Chadormalu deposit, from this study. They represent alkaline- subalkaline (or bimodal) composition, Fe-enrichment tholeiitic series (used diagrams are from Pearce and Cann[59]; Cox *et al.*[79]; Irvin and Baragar[39]; Miyashiro[45]; Jensen *et al.*[42]). (b) Rock types, compositions and suites at Bafq region (Chadormalu, Esfordy) with similar trends in this study; from Isfahani and Sharifi[40]; Ramezani and Tucker[63].

Fig. 2a

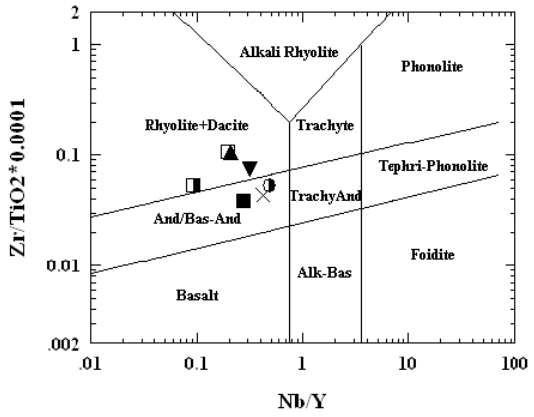
Alkali Rhyolite
Phonolite
Rhyolite+Dacite
Trachyte
Tephri-Phonolite
TrachyAnd
And/Bas-And
Foidite
Alk-Bas
Basalt
Zr/TiO2*0.0001
Nb/Y

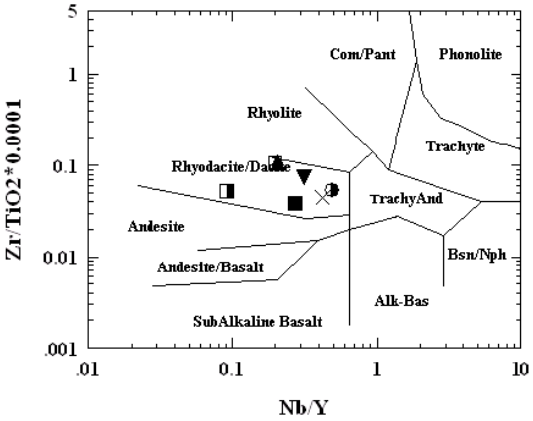
Com/Pant
Phonolite
Rhyolite
Trachyte
Rhyodacite/Dacite
TrachyAnd
Andesite
Bsn/Nph
Andesite/Basalt
Alk-Bas
SubAlkaline Basalt
Zr/TiO2*0.0001
Nb/Y

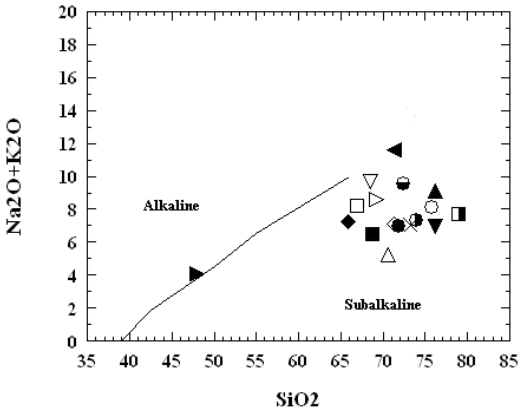
Alkaline
Subalkaline
Na2O+K2O
SiO2

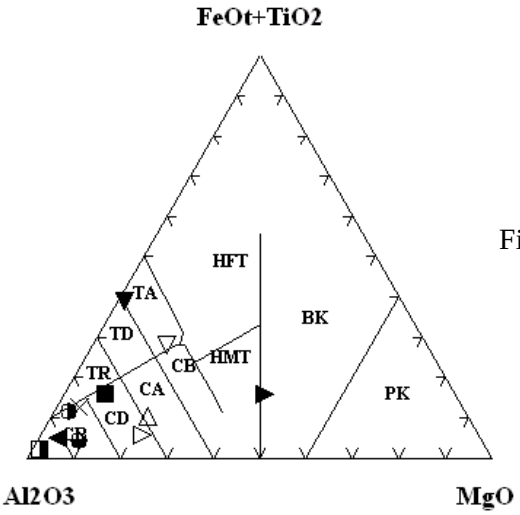
FeOt+TiO2
HFT
TA
BK
TD
CB
HMT
TR
CA
PK
CD
RB
Al2O3
MgO

Fig. 2b

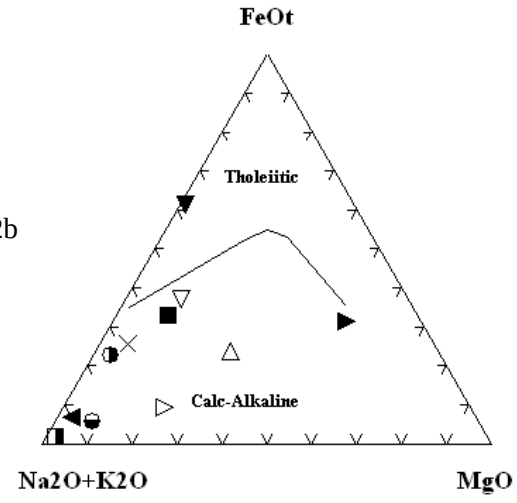
FeOt
Tholeiitic
Calc-Alkaline
Na2O+K2O
MgO

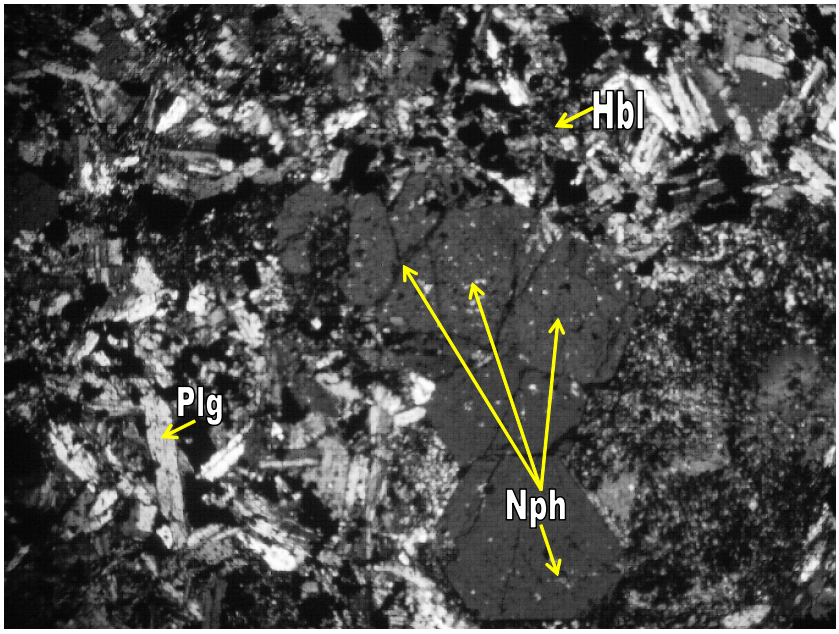

Fig. 3a

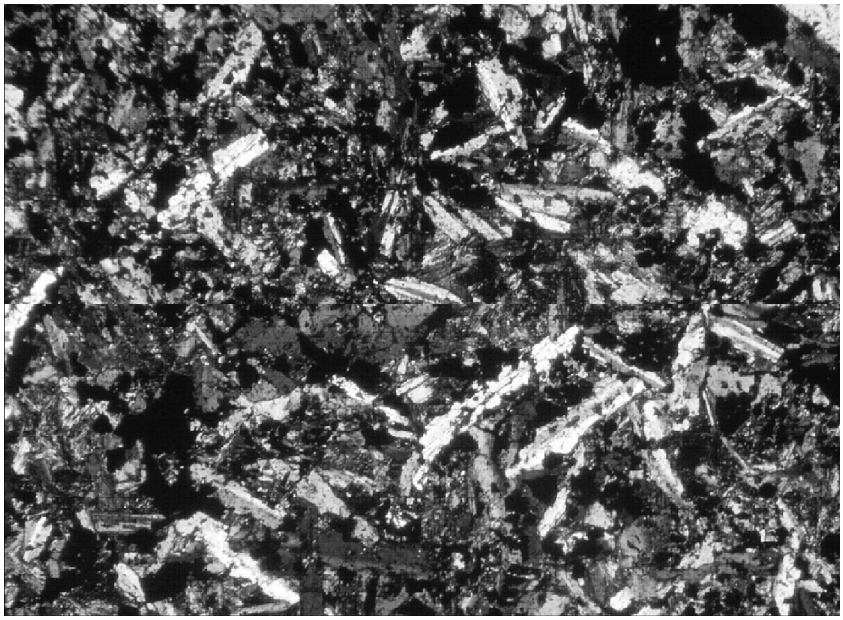

Fig. 3b

Fig. 3 (a & b) Sodic phonolite at Chadormalu ore deposit with undersaturated composition. (c & d) In addition to subalkaline compositions, alkali granite at Chadormalu ore deposit shows an alkaline composition.

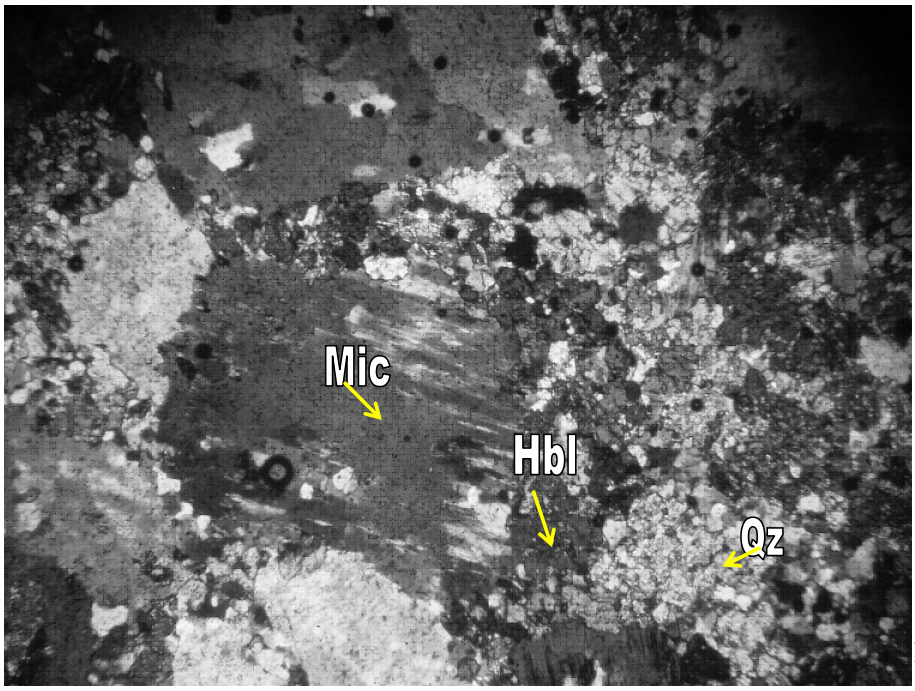

Fig. 3c

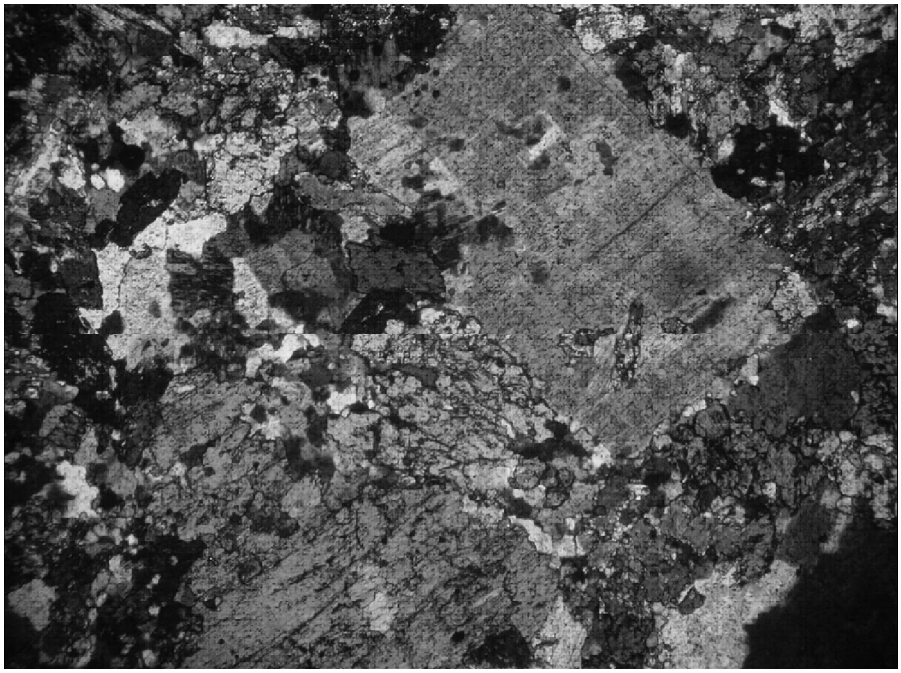

Fig. 3d

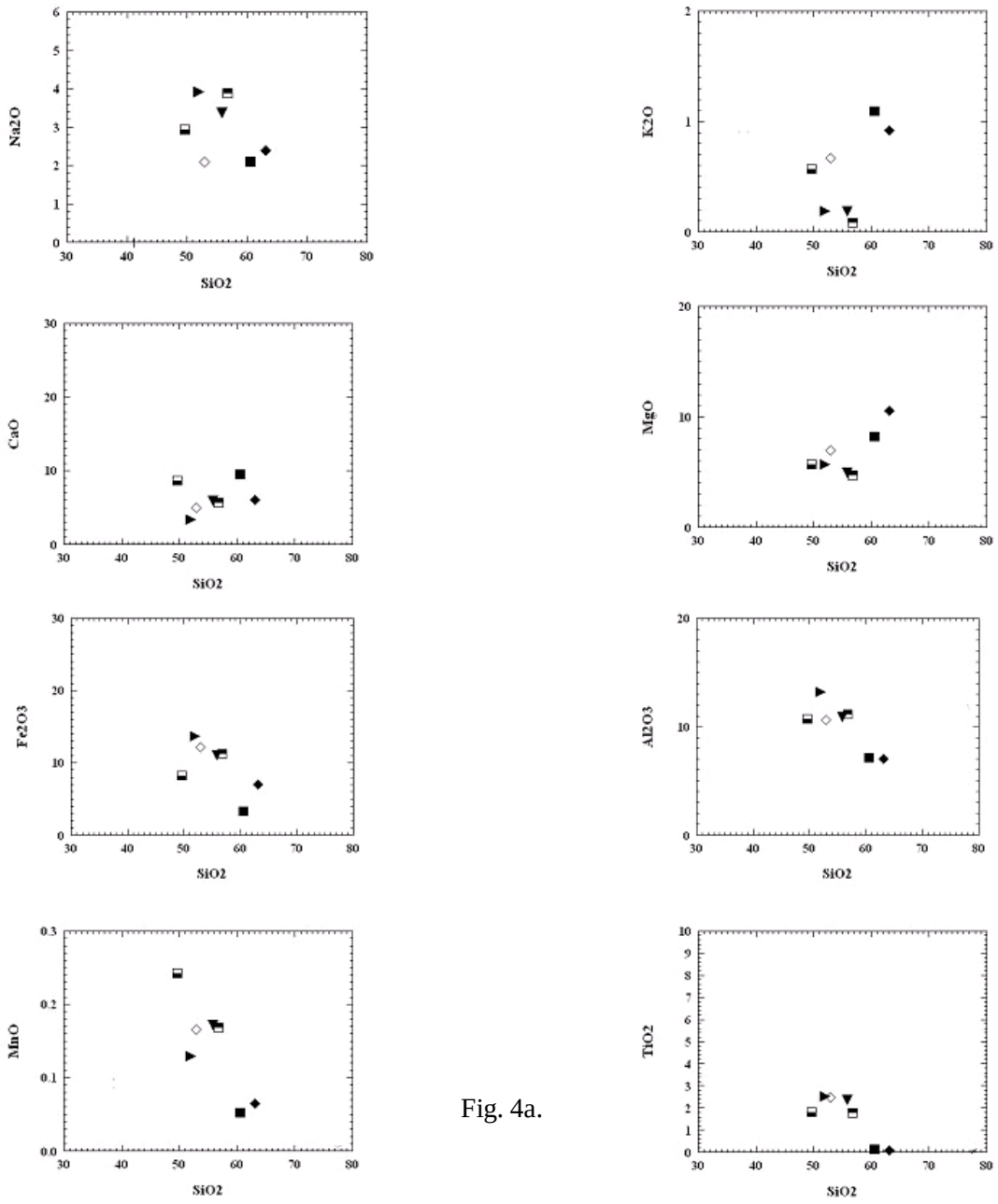

Fig. 4a.

Fig. 4 (a) Harker diagrams of Chadormalu host rocks. They indicate a magmatic suite at Chadormalu deposit. (b) Magmatic series of Bafq region iron host rocks (Chadormalu, Esfordy); from Isfahani and Sharifi [40]; Ramezani and Tucker [63].

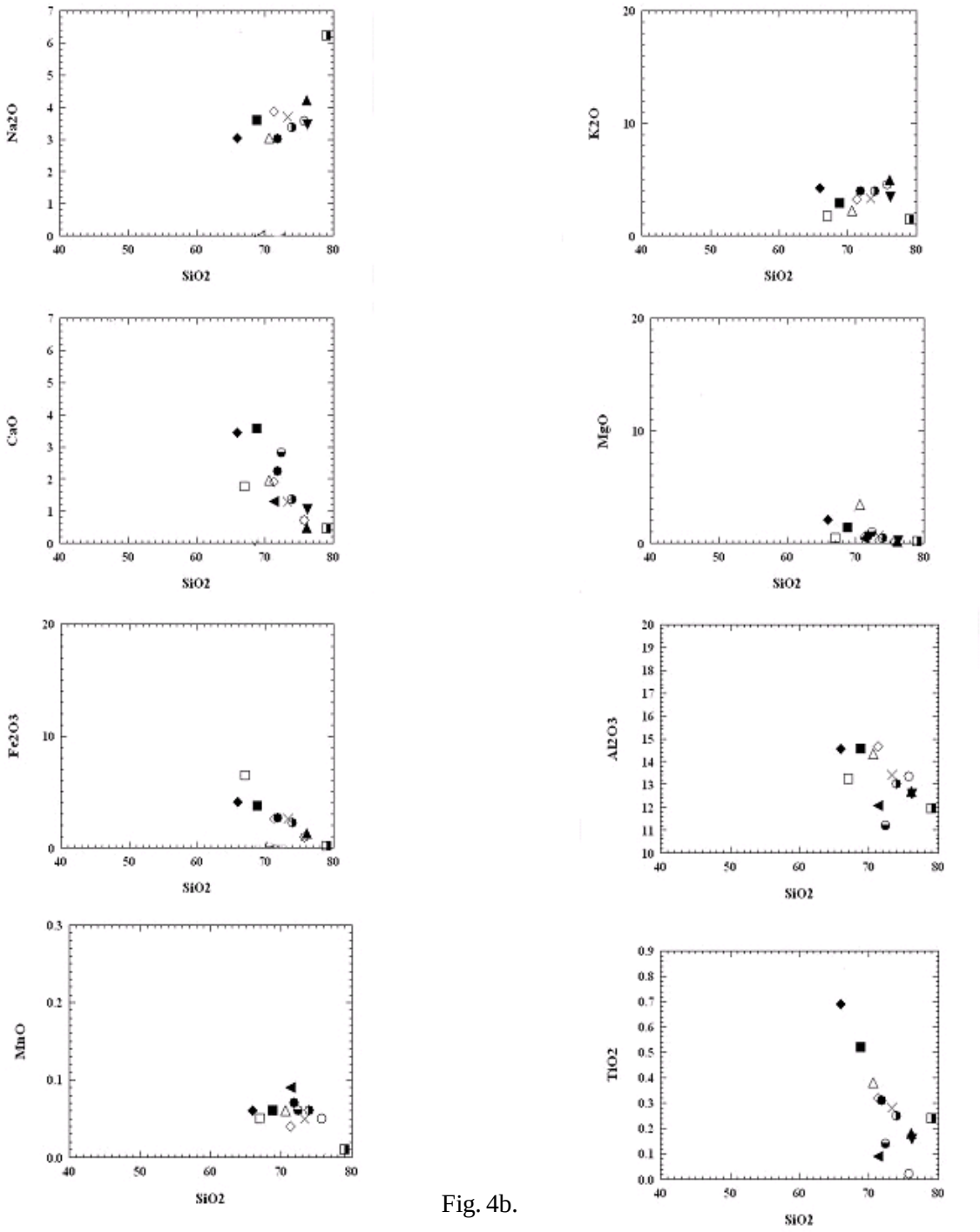
Na2O
SiO2
K2O
SiO2
CaO
SiO2
MgO
SiO2
Fe2O3
SiO2
Al2O3
SiO2
MnO
SiO2
TiO2
SiO2

Fig. 4b.

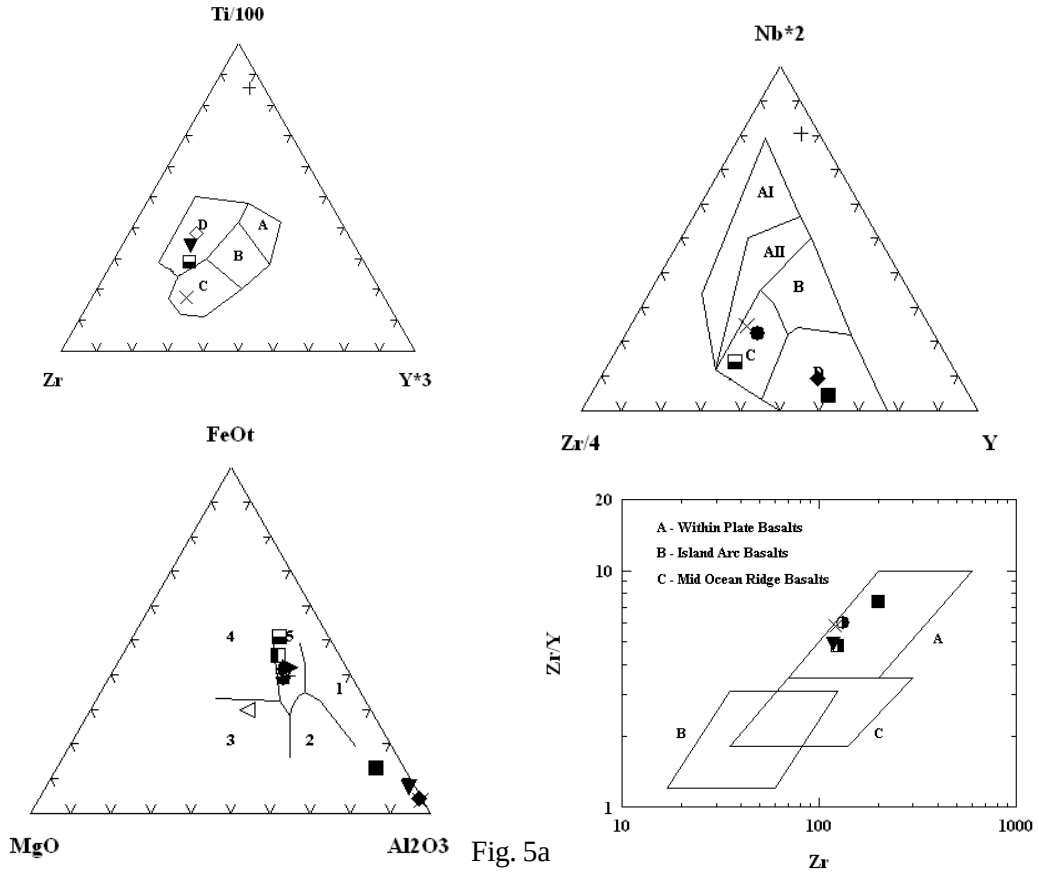

Fig. 5a

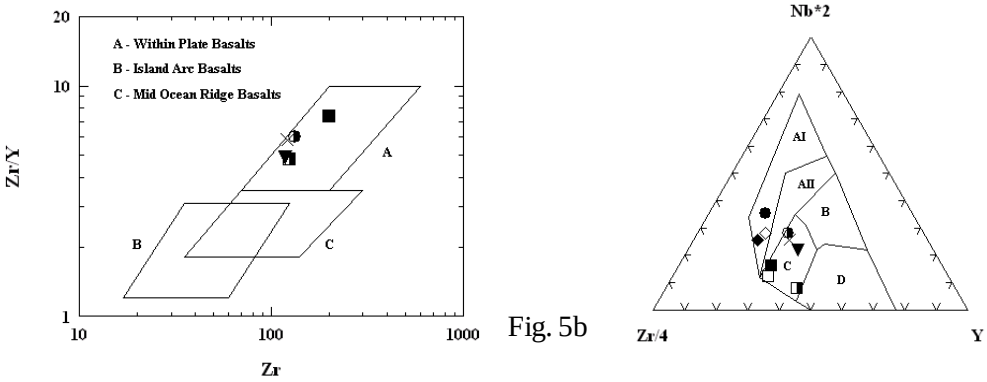

Fig. 5b

Fig. 5(a) within plate and continental setting of Chadormalu iron host rocks (used diagrams are from Pearce and Cann [59]; Pearce and Norry [62]; Pearce et al. [60]; Meschede [44]). (b) Within plate environment of iron host rocks of Bafq region; from Isfahani and Sharifi [40]; Ramezani and Tucker [63].

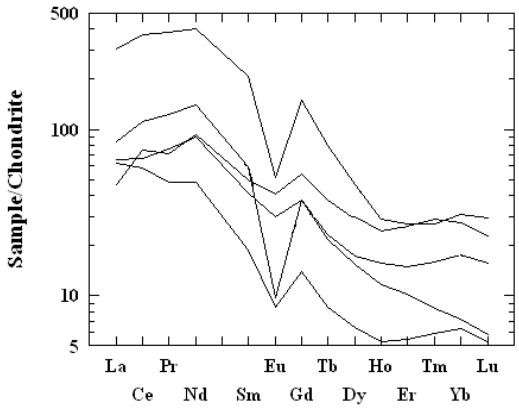

Fig. 6a

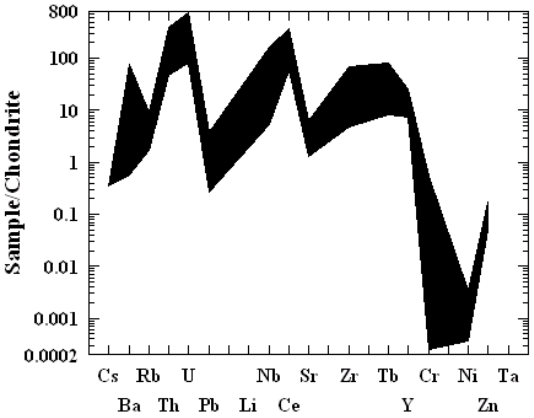

Fig. 6c

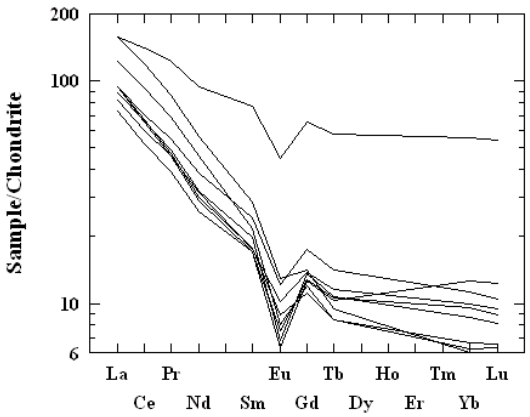

Fig. 6b

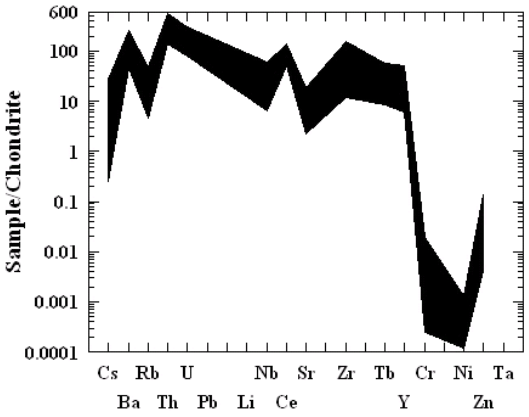

Fig. 6d

Fig.6(a) REE pattern of Chadormalu iron host rocks. This pattern revealed a nonorogenic or continental environment. (b) REE pattern at Bafq region; from Isfahani and Sharifi [40]; Ramezani and
Tucker [63]. Similarly, they indicate a nonorogenic environment. (c) The negative anomaly of Cr, Ni and Nb at Chadormalu host rocks, which, suggests a nonorogenic setting.(d) The similar pattern of Nb, Cr, Ni at Bafq region; from Isfahani and Sharifi [40]; Ramezani andTucker [63].

include coarse volcaniclastic and lacustrine deposits. There is little evidence of evaporites. Such a tectonic environment usually is derived from crustal melting associated with mantle underplating and mantle-derived magmas. Underplating is probably produced by incipient or aborted rifting, mantle hot spot movement, or low angle subduction. Many have magnetite-apatite deposits (Kiruna-type, e.g. Chadormalu deposit),[25,37,38].

A conceptual conclusion by Hitzman *et al*.[38] (on the basis of Forster and Knittle's data, 1979), suggests an extensional environment at the Bafq- region. According to Aghanabati[1],

Upper Precambrian- Lower Cambrian volcanic rocks in Bafq region are alkaline and reflect a continental rift. In the absence of distinguishable contact between Late-Precambrian volcanicevaporite deposits and Early-Cambrian formations Aghanabati[1] suggests a Late-Precambrian to Early-Cambrian age, extending into Middle Cambrian. Samani[72], proposed an intra-continental rift facies (Saqand Formation), comprising five members with different lithologies and bimodal volcanism. According to Momenzadeh[48] and Feiznia[19] volcanic activity introduced ions and volatile components in an early rift basin and evaporate deposition occurred during an early to intermediate rifting stage. The alkaline-sub alkaline volcanism occurred at a later stage. It should be noted that, the introduced ions (e.g. Na+, Cl-, SO42- …) are not evaporative but rather saturated materials, invaded by volcanic vents within the depositional basin. Moore and Modabberi[50] also proposed bimodal volcanism and immature nonmarine clastic sediments in an anorogenic continental rift. The sediments are mostly arkose, quartzite and conglomerate, suggesting under-saturated magmatic rocks (e.g. sodic phonolite at Chadormalu deposit) in continental rift bimodal suites.

Emami[18], proposed a within plate magmasim at the Chadormalu-Saqand area. Again, a nonorogenic continental rift environment associated with tholeiitic, alkaline-subalkaline or undersaturated-saturated or bimodal volcanism; and LREE enrichment[25,43,50]. According to Hall[32] and Raymond[64], in those island arcs that are not underlained by continental crust, andesites are associated with abundant basalts (e.g. shoshonitic basalts) and scarce dacites and rhyolite, but, in volcanic regions underlained by continental crust, they are associated with less abundant basalts and voluminous dacites and rhyolites; in other words, unlike orogenic belts, where intermediate igneous rocks are commonplace, the anorogenic continental areas are characterized by a bimodal association of rhyolite and basalt, or granite and gabbro; that is, continental rift basalts typically are accompanied by more siliceous volcanic rocks ranging from andesite to rhyolite in composition, but the volcanic rock suites are commonly bimodal consisting mainly of two basalt and rhyolite types. Sillitoe[75], proposed that, in arc environments (e.g. IOCG deposits), there are shoshonitic basalt, basalt, basaltic andesite and high K calc-alkaline series, dominantly; but dacite and rhyolite are rare. In other words there is a tholeiitic- calc-alkaline bimodal composition at these environments. Contrary, alkaline-sub alkaline bimodal suites occur in anorogenic continental rift settings[25,32,43,50,64,78]. Island arc basalts are more similar to oceanic island basalts (OIB) than to ocean ridge basalts (MORB). Compared to OIB, they have low contents of

high field strength elements (HFSE) such as Ti, Nb and Ta and high boron. The continental rift basalts are not usually MORB-like. Instead many are similar to ocean island basalts[32,64], (Fig. 6c, d); thus one must be extremely cautious when discriminating tectonic settings.

The collected evidences in this study show that the host rocks (bimodal series) contain voluminous intermediate-felsic intrusive and extrusive rocks (andesite- dacite- rhyolite) with lesser mafic igneous rocks, *i.e.* nonorogenic environment (B-type), suggested by Hitzman[37]. It is only in the rare non orogenic examples that the trend from basalt towards intermediate or acid magma undergoes a degree of Fe-enrichment[9,32]. The Chadormalu host rocks are mostly Fe-enriched tholeiitic rocks (Fig. 2a, b). The normal orogenic andesites are not significantly enriched in Fe compared with associated basalts. The continental volcanic rocks are enriched in alkaline elements, LILE (e.g. Rb, K, Ba, and LREE), volatiles (CO2) and halogens (Cl, F) [43,50]. The concentrations of these elements at the study area (e.g. Chadormalu) are high, especially, LREE, Cl, and F (Table 1). REE patterns at the Bafq host rocks show a LREE-enrichment or a high LREE/HREE ratio (20- 400 times of that of chondrite) (Fig. 6a, b); Eu anomaly varies from slightly negative in andesite to highly negative in felsic rocks; (La/Lu) cn= 1.84- 3.01; ΣREE=198.1- 240. According to Henderson[35] and Raymond[64], these characteristics belong to nonorogenic andesites of continental type. Raymond[64], proposed that, low potassium andesite arcs, boninites and mid oceanic types have low LREE/HREE ratios. Henderson[35] suggested that, Slight Eu anomaly in andesites is indicative of the Pre-Cambrian- Phanerozoic. This author believes that, the HREE depletion is derived from continental (nonorogenic) CO2 degassing.

Mostly, the Ba/Ta ratio in the Bafq area host rocks (e.g. Chadormalu, in this study) is less than 450. Gill[28] demonstrated that, the Ba/Ta ratioe ≥ 450 belongs to arc magmatism. Regarding the spatial and temporal aspects of mineralization it is already well established that, iron oxide (Cu-U-Au-REE) deposits (*i.e.* Kiruna-type - Olympic Dam-type continuum) are associated with anorogenic intrusions between 2000-1000 Ma or Proterozoic Eon[4,65]. The Proterozoic Eon spans a vast period of geological time, from 2500 to 540 Ma, including the period between 2000 and 1000 Ma that is marked with relative paucity of orogenic and/ or magmatic-hydrothermal deposit types, but abundant ores hosted in intra-continental sedimentary basins and anorogenic igneous complexes. These ore forming processes point to a pattern in which a substantial part of Proterozoic crustal evolution was characterized by relatively long-lived periods of continental stability[52,65,81]. According to Sawkins[73], Windley[80,81] and Robb[65], the Paleozoic era was not accompanied by a prolific development of mineralization, since, either the metal contents of crust, were consumed into mineralization at Archean and Protrozoic Eons or ore forming processes has a low activity at this time, or, the erosional and weathering processes in latter eras (Mesozoic and Cenozoic) destroyed them. Dickin[17] suggested that Proterozoic mantle lithosphere has higher level of FeO and other fertile components.

On the basis of all presented evidence, (*i.e.* voluminous felsic intrusive and extrusive rocks with lesser mafic types, bimodal rocks, under saturated-supersaturated silica, or,

tholeiitic, alkalinesub alkaline compositions, extensive sodic and potassic alterations, lagoonal or continental sedimentary sequences, absence of boron (boron depleted), REE contents and patterns, Ba/Ta ratio < 450 and ε Nd amounts), the most probable environment for Bafq area and the associated iron deposits is a nonorogenic continental setting.

The Bafq region metallogenic characteristics (including the Chadormalu and Esfordy deposits) are very similar to Proterozoic Eon (ore forming related to nonorogenic magmatism). Previous studies, proposed 554-531.4 Ma ages (Early-Cambrian) for iron host rocks at the Bafq region, especially, the Chadormalu deposit. The results of this study propose 1-1.3 Ga (Late-Proterozoic) for Chadormalu deposit. In other words, this study suggests an iron mineralization at the Precambrian-Cambrian boundary. Therefore, metallogenically the proposed Infracambrian term is a convenient one. Naturally, it has a hybrid concept (Precambrian-Cambrian metallogenic characteristics, especially, late or neo-Proterozoic era). Comparison of Proterozoic and Phanerozoic metallogenic characteristics indicates that, the iron deposits of the Bafq region belong to late (Neo) Proterozoic- Early Cambrian boundary.

Acknowledgment

This study was financially supported by the Shiraz University and payam-e- Noor University research councils to whom we are indebted. The Authors extend their thanks to Prof. Hitzman of C.S.M for constructive comments.

References

1. Aghanabati, A., Geology of Iran. 586, Geological Survey of Iran, (In Farsi) (2004).
2. Allegre, C. J., Hart, S. R., Mister, J. F., Chemical structure and evolution of the mantle and continents determined by inversion o Nd and Sr isotopic data, II. Numerical experiments and discussion. Earth planetary of Science Letters 66, 191-213 (1983a).
3. Archer, A., Schmidt, U., Mineralized breccias of early Proterozoic age, Bonnet Plume River district, Yukon Territory. Canadian Institute of Mining and Metallurgy Bulltain *71*, 53-58 (1978).
4. Barley, M. E., Groves, D.I., Supercontinent cycles and distribution of metal deposits through time. Geology *20*, 291-294 (1992).
5. Barton, M. D., Johnson, D. A., Evaporitic-source model for igneous-related Fe oxide-(REE-Cu-Au-U) mineralization. Geology *24*, 259-262 (1996).
6. Bohne, E., Aber blick ader blick ader die Erzlagerstatten persiens and den derzeitigen stand Von Gewinnang and Verhuttung. Mettall and Erz *26*, 57 – 61 (1929).
7. Bookstrom, A. A., The magnetite deposits of El Romeral, Chile. Economic Geology *72*, 1101-1130 (1977).
8. Borook, D.M., Kesler, S.E., Boer, R. H., Essene, E.J., Vergenoeg magnetite-flourite deposit, South Africa: support for a hydrothermal model for massive iron oxide deposits. Economic Geology *93*, 564-586 (1998).
9. Carmichael, I. S. E., The petrology of Thingmuli, a Tertiary volcano in eastern Iceland. Journal of petrology *5*, 435-460 (1964).
10. Cox, K. G., Bell, J. D., Pankhurst, R. J., The interpretation of igneous rocks. George Allen and Unwin. Press, London, 396p

(1979).
11. Daliran, E., The magnetite–apatite deposit of Mishdovan, East central Iran, An alkali rhyolite hosted, Kiruna type, occurrence in the Infracamdrian Bafq metallotect. Germany. Ph.D. thesis, Heidelberger Geowissensch, aftliche Abhandelungen, 37, 248 p (1990).
12. Daliran, F., REE geochemistry of Kiruna–type iron ores. In: Stanley, C. J., Rankin, A.H., Bondar, R.J. (Eds.), Mineral Deposits, Processes to Processing, Balkema, Rotterdam, *1*, 631 – 634 (1999).
13. Daliran, F., Kiruna – type iron oxide – apatite ores and apatites of the Bafq district, Iran. With an emphasis on the REE geochemistry of their apatites. In: Porter, T.M. (Eds.), Hydrothermal iron oxide copper – Gold – a related deposits: A Global prospective, volume I, PGC publishing, Adelaide, 303-320 (2002).
14. Daliran, F., Amstutz, G.C., The magnetite–apatite deposit of Mishdovan: An alkali rhyolite, hosted Kiruna type ore in the Bafq metallotect, east central Iran. In: Jafarzadeh, A. (eds.) Conference on Ore Deposits of Yazd Province, Ministry of Mining *1*, 22-26 (1991).
15. Daliran, F., Stosch, H.G., Geology and metallogenesis of the phosphate and rare earth element resources of the Bafq iron-ore district, central Iran. In: Jafarzadeh, A. (eds.), World Mining Congress and Exploration. 20th, 11-6 (2005).
16. Davidson, J.P., Crustal contamination versus subduction zone enrichment: Examples from the Lesser Antilles and implications for mantle source compositions of island arc volcanics. Geochimica et Cosmochemica Acta *51*, 2185-2198 (1987).
17. Dickin, A.P., Radiogenic isotope geology. Cambridge University Press, London, 492p (2005).
18. Emami, M.H., Magmatism in Iran. Geological Survey of Iran, Tehran, 608 p (In Farsi) (2000).
19. Feiznia, S., Non-terigenous sedimentary rocks (excluding carbonates). Tehran University Publications, 262 p (In Farsi) (1993).
20. Forster, H., Borumandi, H., Jungprekambriseh magnetite lava and magnetite tuff aus dem zenral Iran.Naturwissen schaften 58, 10, 524-541 (1971).
21. Forster, H., Jafarzadeh, A., The Chadormalu iron ore deposit (Bafq district, central Iran) – magnetite filled pipes. Neues Jahrbuch für Geologie und Palaontologie, Abhandlungen *168*, 524 – 534 (1984).
22. Forster, H., Jafarzadeh, A., The Bafq mining district in central Iran – a highly mineralized Infracambrian volcanic field. Economic Geology *89*, 1697–1721 (1994).
23. Forster, H., Knittel, U., Petrographic observations on a magmatic deposit at Mishdovan, central Iran. Economic Geology *74*, 1485-1510 (1979).
24. Frietsch, R., On the magmatic origin of iron ores of the Kiruna type. Economic Geology *73*, 478-485 (1978).
25. Frietsch, F., Perdahl, J.A., Rare earth elements in apatite and magnetite in Kiruna-type iron ores and some other iron ore types. Ore Geology reviews *9*, 489-510 (1995).
26. Geijer, P., Odman, O.H., The emplacement of the Kiruna iron ores and related deposits. Sveriges Geol. Undersokning. Ser. C 700, 48 pp (1974).
27. Gerasimovskiy, V.V., Mineve, D.A., Redkozemelyne element apatitach or apatit-magnetiovch. Rud. Geochimija *1*,

99-104 (1981).
28. Gill, J.B., Orogenic andesites and plate tectonics. Springer-Verlag, Berlin, 390p (1981).
29. Guilbert, J. M., Park, C. F., The geology of ore deposits. Freeman, New York, 985p (1997).
30. Haghipour, A., Etude geologique de la region de Biabanak – Bafq (Iran central): Petrogrephic et tectonique du socle precambrien et de SA couverture. Ph.D. thesis, de' Etad. University of groenoble. France, 403 p (in French) (1974).
31. Halalat, H., Bolurchi, M. H., Phosphate deposits. Geological Survey of Iran, Tehran, 200p (1995).
32. Hall, A., Igneous petrology. Addison Wesley, London, 551p (1998).
33. Hamdi, B., Precambrian-Cambrian deposits in Iran. Geological Survey of Iran, Tehran, 364 p (1995).
34. Haynes, D. W., Cross, K. C., Bills, R. T., Reed, M. H., Olympic Dam ore genesis: a fluid-mixing model. Economic Geology *90*, 281-307 (1995).
35. Henderson, P., Rare earth element geochemistry. Elsevier Publication, Amsterdam, 510 p (1989).
36. Hildebrand, R.S., Kiruna-type deposits: their origin and relationship to intermediate subvolcanic plutons in the Great Bear Magmatic Zone, Northwest Canada. Economic Geology *81*, 640-659 (1986).
37. Hitzman, M.W., Iron oxide-Cu-Au deposits: what, where, when and why. In: Porter. T.M. (Ed). Hydrothermal iron oxide copper-gold and related deposits: A global perspective. Australia Mineral Foundation, Adelaide, 9-25 (2000).
38. Hitzman, M.W., Oreskes, N., Enaudi, M., Geological characteristics and tectonic setting of Proterozoic iron oxide (Cu – U–Au – REE) deposits. Precambrian Research *58*, 241 – 287 (1992).
39. Irvine, T. N., Baragar W. R. A., A guide to the chemical classification of the common volcanic rocks. Canadian Journal of Earth Sciences, *8*, 523-548 (1971).
40. Isfahani, F., Sharifi, A., Geochemical characteristics of magmatic rocks of Iran. Geological Survey of Iran, Tehran, *2*, 1464p (1999).
41. Jafarzadeh, A., Die manenetiterzlager-statte chadormalu in zentralion and ihre exploration. Ph.D. thesis. Germany. Rheinishe – Westfalische Techniche. Hochshale, 152 p (in Germany) (1981).
42. Jensen, L.S., A new cation plot for classifying subalkalic volcanic rocks. Ontario Div. Mines. Misc, 1, 66p (1976).
43. Kearey, P., Vine, F. J., Global tectonics. Blackwell Publication, London, 220 p (1996).
44. Meschede, M., A method of discriminating between different types of mid ocean ridge basalts and continental tholeiites with the Nb-Zr-Y diagrams. Chemical Geology *56*, 207-218 (1986).
45. Miyashiro, A., Volcanic Rock Series and Tectonic Setting. Anniversary Review of Earth Planetary Sciences, *3*, 251-269 (1975).
46. Moghtaderi, A., Moore, F., Remote sensing of structural features associated with iron-apatite mineralization in Bafq paleorift, central Iran. Journal of Ultra Scientist of Physical Sciences *19*, 11-26 (2007).
47. Moghtaderia, A., Moore, F., Mohammadzadeh, A., The application of advanced space-borne thermal emission and reflection (ASTER) radiometer data in the detection of alteration in the Chador-

malu paleocrater, Bafq region, Central Iran. Journal of Asia Earth Sciences *30*, 238-252 (2007).

48. Momenzadeh, M., Saline deposits and alkaline magmatism, a genetic model. Geological survey of Iran *45*, 1385-1495 (1987).
49. Moore, F., Modabberi, S., Origin of Choghart iron oxide deposit, Bafq mining district, central, Iran: new isotopic and geochemical evidences. Journal of Scientific of Islamic Republic of Iran *14*, 259-269 (2003).
50. Moore, F., Modabberi, S., Plate tectonic and geological processes. Kooshamehr Publications, Shiraz, 467p (In Farsi) (2002).
51. Mucke, A., younessi, R., Magnetite-apatite deposits (Kiruna- type) along the Sanandaj- Sirjan zone and in the Bafq area associated with ultramafic and calcalkaline rocks and carbonatites. Contribution to Mineralogy and Petrology *50*, 219-244 (1994).
52. Nance, R. D., Worsley, T. R., Moody, J.B., Post Archean biogeochemical cycles and long-term episodicity in tectonic processes. Geology *14*, 514-518 (1986).
53. NISCO (National Iranian steel corporation), Report on results of search and valuation works at magnetic anomalies of the Bafq iron are region during 1976-1979, 89, 260 p (1980).
54. Nohda, S., Wasserburg, G. J., Nd and Sr isotopic study of volcanic rocks from Japan. Earth and Planetary Science Letters 52, 2, 264-276 (1981).
55. Nystrom, J. O., Henriquez, F., Magmatic features of iron ores of the Kiruna type in Chile and Sweden: ore textures and magnetite geochemistry. Economic Geology *89*, 820-839 (1994).
56. Panno, S. V., Hood, W., Volcanic stratigraphy of the Pilot Knob iron deposits, Iron Country, Missouri. Economic Geology 78, 972-982 (1983).
57. Parak, T., Kiruna iron ores are not intrusive-magmatic ores of the Kiruna type. Economic Geology *70*, 1242-1258 (1975).
58. Park, C.F., The iron ore deposits of the Pacific basin. Economic Geology *67*, 339-349 (1972).
59. Pearce, J.A., Cann, J.R., Tectonic setting of basic volcanic rocks determined using trace element analyses. Earth Planetary Science Letter *19*, 290-300 (1973).
60. Pearce, T.H., Gorman, B. E., Birkett, T.C., The relationship between major element chemistry and tectonic environment of basic and intermediate volcanic rocks. Earth Planetary Science Letter *36*, 121-132 (1977).
61. Pearce, J. A., Harris, N. B. W., Tindle, A. G., Trace element discrimination diagrams for the tectonic interpretation of granitic rocks. Journal of Petrology *25*, 956-983 (1984).
62. Pearce, J. A., Norry, M. J., Petrogenetic implications of Ti, Zr, Y and Nb variations in volcanic rocks. Contribution to Mineralogy and Petrology *69*, 33-47 (1979).
63. Ramezani, J., Tucker, R. D., The Saqand region, central Iran: U-Pb Geochronology, Petrogenesis and Implications for Gondwana Tectonics. American Journal of Sciences *303*, 622-665 (2003).
64. Raymond, L. R., Petrology: The study of igneous sedimentary and metamorphic rocks. McGraw-Hill, Boston, 720p (2002).
65. Robb, L., Introduction to ore-forming processes. Blackwell publishing, Hong Kong, 373 p (2005).
66. Rollinson, H. R., Using geochemical data:

evaluation, presentation, interpretation. Longman Publisher, London, 225 p (1993).
67. Rosiere, C. A., Rios, F. J., The origin of hematite in high-grade iron ores based on infrared microscopy and fluid inclusion studies: the example of the Conceicao mine, Quadrilater Ferrifero, Brazil. Economic Geology *99*, 611-624 (2004).
68. Ryan, J. G., Langmuir, C. H., The Systematic of boron abundances in young volcanic rocks. Geochemica et Cosmochemica Acta *57*, 1489-1498 (1993).
69. Samani, B.A., Precambrian metallogenic deposits in central Iran. AEOI, Scientific Bulletin 17, 1-16 (in Farsi with English abstract) (1998).
70. Samani, B., Zhuri, G., Zuetao, G., Chuna, T., Geology of Precambrian in central Iran; on the context of stratigraphy, magmatism, and metamorphism. Geosciences Scientific Quarterly Journal, Geological Survey of Iran 3, 10, 40- 63 (In Farsi with English abstract) (1994).
71. Samani, B., Saqand formation, a riftogenic unit of upper Precambrian in central Iran. Geosciences Scientific Quarterly Journal, Geological Survey of Iran 2, 6, 32–45 (in Farsi with English abstract) (1993).
72. Samani, B., Metallogeny of the Precambrian in Iran. Precambrian Research *39*, 85 – 106 (1988).
73. Sawkins, F. J., Sulfide ore deposits in relation to plate tectonics. Journal of Geology *80*, 377-379 (1972).
74. Schwartz, M. O., Melcher, F., The Flame Iron District, Senegal. Economic Geology *99*, 917-939 (2004).
75. Sillitoe, R. H, Iron oxide-copper-Gold deposits: an Andean View. Mineralium Deposita *38*, 787-812 (2003).
76. Snyder, F.G., Precambrian iron deposits in Missouri. Economic Geology *4*, 231-238 (1969).
77. Taylor, R. P. and Fryer, B. J., Multi-stage hydrothermal Alteration in porphyry copper systems in northern Turkey: the temporal inter play of potassic, propylitic, and phylic fluids. Canadian Journal of Earth Sciences, *17*, 901-926 (1980).
78. Thorpe, R.S., Smith, K., Mid plate volcanism in Geodynamics today, a review of the earth's dynamic processes. Royal Society of London, 75-80 (1975).
79. Williams, G.H., Hushmandzadeh, A., A pertrological and genetic study of the Choghart iron are body and the surrounding rocks. Geological Survey of Iran, *2*, 18p (1966).
80. Windley, B. F., The evolving continents. John Wiley and Sons, New York, 385 p (1978).
81. Windley, B. F., The evolving continents. John Wiley and Sons, New York, 526 p (1995).
82. Wood, D. A., The application of a Th-Hf-Ta diagram to problems of tectonomagmatic classification and establishing the nature of crustal contamination of basaltic lavas of the British Tertiary volcanic province. Earth Planetary Science Letter *50*, 11-30 (1980).